Editors' Suggestion | Featured in Physics

Universal Relation between Instantaneous Diffusivity and Radius of Gyration of Proteins in Aqueous Solution

Eiji Yamamoto,[1,*] Takuma Akimoto,[2] Ayori Mitsutake,[3] and Ralf Metzler[4]
[1]Department of System Design Engineering, Keio University, Yokohama, Kanagawa 223-8522, Japan
[2]Department of Physics, Tokyo University of Science, Noda, Chiba 278-8510, Japan
[3]Department of Physics, Meiji University, Kawasaki, Kanagawa 214-8571, Japan
[4]Institute of Physics and Astronomy, University of Potsdam, 14476 Potsdam-Golm, Germany

(Received 5 September 2020; accepted 9 February 2021; published 23 March 2021)

Protein conformational fluctuations are highly complex and exhibit long-term correlations. Here, molecular dynamics simulations of small proteins demonstrate that these conformational fluctuations directly affect the protein's instantaneous diffusivity D_I. We find that the radius of gyration R_g of the proteins exhibits $1/f$ fluctuations that are synchronous with the fluctuations of D_I. Our analysis demonstrates the validity of the local Stokes-Einstein–type relation $D_I \propto 1/(R_g + R_0)$, where $R_0 \sim 0.3$ nm is assumed to be a hydration layer around the protein. From the analysis of different protein types with both strong and weak conformational fluctuations, the validity of the Stokes-Einstein–type relation appears to be a general property.

DOI: 10.1103/PhysRevLett.126.128101

Diffusion of colloidal particles in a bulk liquid, known as Brownian motion, is driven by collisions with the surrounding liquid molecules. Its ensemble-averaged mean squared displacement (MSD) $\langle \boldsymbol{r}(t)^2 \rangle = 2dDt$ grows linearly with time, where d is the spatial dimension, $\boldsymbol{r}(t)$ is the particle position, and D is the diffusion coefficient. In a high-viscous liquid, D of a spherical particle of radius R follows the classical Stokes-Einstein (SE) relation $D = k_B T/6\pi\eta R$, where η is the viscosity and $k_B T$ is the thermal energy. In a coarse-grained view, the radius R of a diffusing particle is typically assumed to be constant.

The SE-type relation is also valid for the diffusion of proteins, $D \propto 1/R_H$, where R_H is the hydrodynamic radius of a protein. The translational diffusivity of isolated proteins in solution has been predicted by its size and shape, e.g., molecular weight [1,2], radius of gyration [2,3], and interfacial hydration [4]. Additionally, complex protein-protein interactions are a determinant factor for protein diffusion in macromolecularly crowded liquids [5,6]. Interestingly, also two-dimensional lateral diffusion of transmembrane proteins in protein-crowded membranes follows a SE-type relation [7], while in protein-poor membranes the protein diffusivity follows the logarithmic Saffman-Delbrück law $D \propto \ln(1/R)$ [8].

Recently, spatial and temporal fluctuations of the local diffusivity of tracer particles have been reported in heterogeneous media, such as supercooled liquids [9], soft materials [10,11], and biological systems [12–20]. The measured tracer dynamics exhibits a non-Gaussian distribution of displacements, anomalous diffusion with a nonlinear t dependence of the MSD, and dynamical heterogeneity. Specifically, the local diffusivity fluctuates significantly with time due to the influence of heterogeneity in the media, e.g., clustering, intermittent confinement, structure variation, etc. Numerous theoretical fluctuating-diffusivity models explain specific features of the non-Gaussianity and anomalous diffusion [21–34].

Interestingly, a fluctuating diffusivity was observed for polymer models in dilute solutions [35]. However, the precise influence of the temporal change of the observed particle itself on the diffusivity fluctuations remains unclear. Protein molecules represent a uniquely suited system to explore the direct connection between instantaneous conformation and diffusivity. Namely, incessant protein conformational fluctuations range from small local conformational changes to large and even global changes in domain motion and in the folding and unfolding dynamics. Since instantaneous conformations are expected to affect the instantaneous diffusivity of the proteins, conformational fluctuations may induce a fluctuating diffusivity of proteins. If true, it is an interesting question to unveil whether a SE-type relation holds between the locally fluctuating diffusivity and the protein conformations while the classical SE relation is established only for a static tracer particle.

Here, we report results from extensive all-atom molecular dynamics (MD) simulations of small proteins isolated in solution to elucidate the effect of protein conformational fluctuation on the protein diffusivity. Specifically, we show that the temporal fluctuations of the instantaneous protein diffusivity D_I *directly* depends on the instantaneous radius of gyration R_g by the SE-type relation $D_I \propto 1/(R_g + R_0)$, where $R_0 \sim 0.3$ nm is assumed to be a hydration layer around the protein.

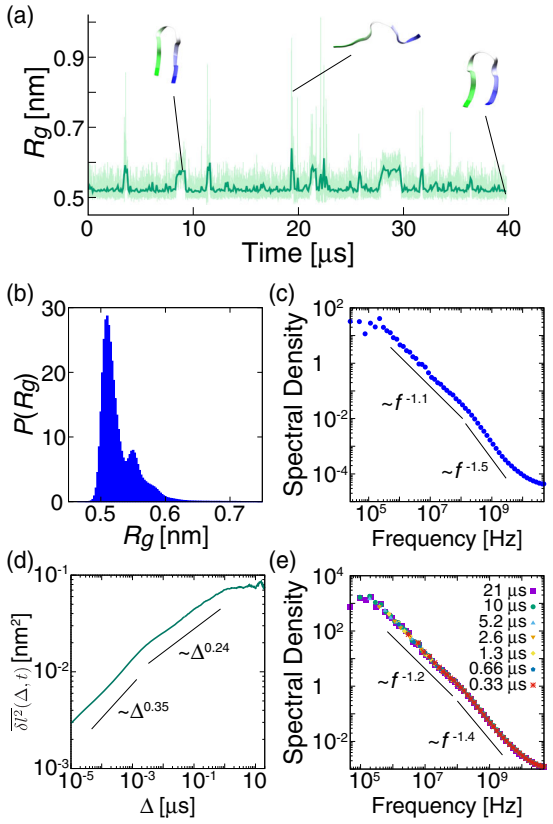

FIG. 1. Conformational fluctuations of Chignolin at 310 K and 0.1 MPa. (a) Time series of the gyration radius R_g. Thin and thick lines represent the unsmoothed original values every 1 ns and a smoothed moving average with 100 ns averaging window, respectively. (b) Probability density function of R_g. (c) Ensemble-averaged PSD of R_g averaged over five trajectories of 40 μs. Solid lines are shown for reference. (d) Ensemble- and time-averaged mean squared protein end-to-end distance for measurement time $t = 40$ μs. (e) Ensemble-averaged PSDs of the end-to-end distance. Different colored symbols represent the PSDs for different measurement times.

Conformational fluctuations of Chignolin.—Five independent simulation runs of the protein super Chignolin [36] were run for 40 μs (see details in Supplemental Material [37]). To evaluate the conformational fluctuations of Chignolin, the radius of gyration, $R_g^2 = N^{-1}\sum_{i=1}^{N}(\boldsymbol{r}_i - \boldsymbol{r}_g)^2$, was calculated, where N is the number of amino acid residues, and $\boldsymbol{r}_i$ and $\boldsymbol{r}_g$ are the entire center of mass positions of the ith residue and the protein, respectively. A time series of R_g is shown in Fig. 1(a). The lower values of R_g correspond to the folded conformations, while the higher value corresponds to the unfolded conformations. The probability density function of R_g shows two peaks at 0.51 and 0.55 nm, which correspond to the native state and metastable (misfolded) state, respectively [see Fig. 1(b)]. Several metastable structures were observed in this simulation of super Chignolin at room temperature (Fig. 2).

Fluctuations of the protein conformations are known to show long-term correlations [51–54]. Chignolin undergoes a folding and unfolding transition on a timescale of microseconds. To elucidate the correlations of the conformational fluctuations, the ensemble-averaged power spectral density (PSD) of R_g was calculated [Fig. 1(c) and Fig. S1 [37]]. The PSD exhibits $1/f$ noise with a power-law exponent of -1.5 at high frequencies and -1.1 at low frequencies, the transition frequency is 2×10^8 Hz. Below a frequency of $\sim 10^6$ Hz, the PSD assumes a plateau, which implies stationarity of the process. The $1/f$ behavior of the PSD is observed for other small proteins, such as Villin and WW domain of Pin1, whose sizes are about 3 times larger than Chignolin, with different power-law exponent (Fig. S2).

The observed PSD transition frequencies correspond to the timescale of conformational protein fluctuations. Indeed the time-averaged mean squared end-to-end distance δl^2 of Chignolin exhibits a sublinear increase with two transition points at ~ 1 ns and ~ 1 μs [see Fig. 1(d), details in Supplemental Material [37]]. These transition times are of the same order as those of the PSD of R_g. The PSDs of the end-to-end distance for different measurement times clearly shows $1/f$ noise similar to that of R_g [Fig. 1(e)]. The consistency of the PSDs for different measurement times implies absence of aging [55–57] (see also Fig. S3). For Chignolin, we clearly see the relaxation of the conformational fluctuations (plateau in the PSD).

To dissect the dynamical modes of the protein, a relaxation mode analysis (RMA) [58–61] was performed (see Fig. 2 and Figs. S4–S8). The free energy maps of relaxation modes (RMs) clearly identify the native state, metastable state, and other states, including unfolded conformations. The slowest mode (mode 1) corresponds to a transition between the native and metastable states. The transition between the native and intermediate states are extracted to the second slowest mode (mode 2). To reveal the origin of the transitions in the PSD of R_g, cumulative PSDs summed over 24 individual PSDs of each RM are shown in Fig. 2(b). The cumulative PSD of RMs shows a similar decay as the PSD of R_g. Note that the power-law scaling exponent of the cumulative PSDs converges from -2 to -1.1 (see Fig. S7). This is because the individual PSDs of each RM are expected to exhibit a Brownian noise ($\propto 1/f^2$) due to its exponential relaxation, and the crossover frequency, at which the PSD assumes a plateau, corresponds to the relaxation time of its exponential relaxation (Figs. S4 and S5). Interestingly, while the cumulative PSD using only the Cα atoms does not show the crossover of the power-law exponents between -1.1 and -1.5 at the transition frequency of 2×10^8 Hz, the cumulative PSD using all heavy atoms does show the crossover; i.e., the crossover at high frequencies originates from the conformational relaxation of side chains. In addition, the slowest RM of the crossover between the

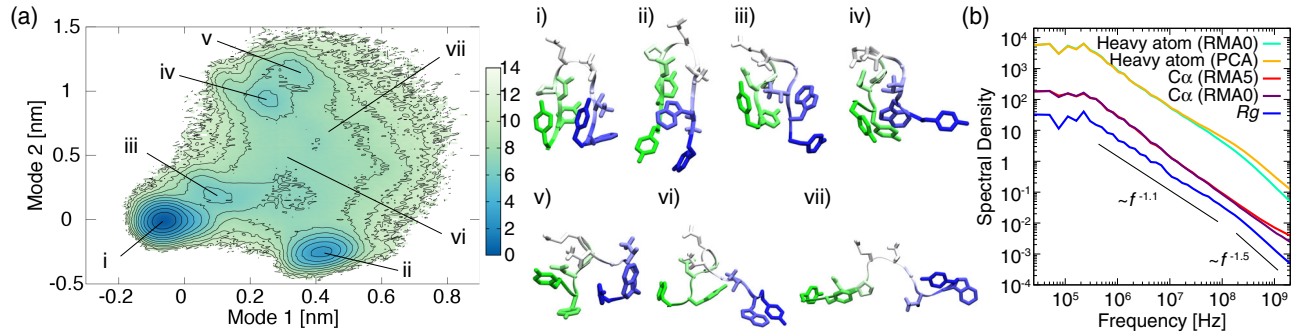

FIG. 2. Decomposition of the relaxation modes of Chignolin at 310 K and 0.1 MPa. (a) Free energy map for the slowest relaxation mode (mode 1) vs the second slowest mode (mode 2) obtained by RMA using the coordinates of Cα atoms with parameters $t_0 = 0.5$ and $\tau = 0.1$ ns. Snapshots of protein conformations corresponding to the free energy maps: (i) native state, (ii) metastable state, and (iii)–(vii) states 3–7. Residues 1–10 are colored green to blue. (b) Ensemble-averaged cumulative PSDs of relaxation modes and principal components. RMA and principal component analysis (PCA) were performed using coordinates of heavy atoms or Cα atoms. Parameters for RMA were set as RMA0 ($t_0 = 0$ and $\tau = 0.1$ ns) and RMA5 ($t_0 = 0.5$ and $\tau = 0.1$ ns).

native and metastable states is related to the crossover frequency where the PSD of R_g assumes a plateau.

Fluctuating diffusivity of Chignolin.—To evaluate the diffusive dynamics of Chignolin in solution, we calculated the time-averaged MSDs,

$$\overline{\delta \boldsymbol{r}^2}(\Delta, t) = \frac{1}{t-\Delta}\int_0^{t-\Delta} \delta \boldsymbol{r}^2(\Delta, t')dt', \tag{1}$$

where Δ is a lag time, t is the measurement time, and $\delta \boldsymbol{r}(\Delta, t') = \boldsymbol{r}(t'+\Delta) - \boldsymbol{r}(t')$ is the displacement vector of the center of mass position of the protein. Some scatter was observed where Δ becomes comparable to t (Fig. S9). To examine the fluctuations of the diffusivity, we calculated the magnitude and orientation correlation functions of the diffusivity [35,37]. The magnitude correlation is defined by

$$\Phi_1(\Delta, t) = \langle |\overline{\delta \boldsymbol{r}^2}(\Delta, t)|^2 \rangle - \langle \overline{\delta \boldsymbol{r}^2}(\Delta, t) \rangle^2, \tag{2}$$

and the dimensionless form $\hat{\Phi}_1(\Delta, t)$ yields from division by $\langle \overline{\delta \boldsymbol{r}^2}(\Delta, t) \rangle^2$. $\hat{\Phi}_1(\Delta, t)$ is equivalent to the ergodicity breaking parameter [23,25,62]. In the case of ergodic diffusion, e.g., Brownian motion, this parameter converges to zero with a power-law decay $\propto t^{-1}$. However, in the case of nonergodic diffusion [63], e.g., continuous-time random walks [62,64,65] and annealed transit time models [66], the magnitude correlation converges to a nonzero value for all $\Delta \ll t$ as $t \to \infty$. The magnitude correlation function $\hat{\Phi}_1(\Delta, t)$ of Chignolin shows a slow decay with scaling exponent below -1, in the time region $t \sim 10^{-2}$–1 μs [Fig. 3(a)]. This implies that the instantaneous diffusivity may fluctuate intrinsically on the corresponding timescales. Note that the power-law decay of -1 at shorter and longer timescales means that the effect of fluctuating diffusivity can be ignored on these timescales. The orientation correlation is defined by

$$\Phi_2(\Delta, t) = \langle \overline{\delta \boldsymbol{r} \delta \boldsymbol{r}}(\Delta, t) : \overline{\delta \boldsymbol{r} \delta \boldsymbol{r}}(\Delta, t) \rangle - \langle \overline{\delta \boldsymbol{r} \delta \boldsymbol{r}}(\Delta, t) \rangle : \langle \overline{\delta \boldsymbol{r} \delta \boldsymbol{r}}(\Delta, t) \rangle, \tag{3}$$

where $\overline{\delta \boldsymbol{r} \delta \boldsymbol{r}}(\Delta, t)$ is a time-averaged MSD tensor [37], a double dot : is defined by $\boldsymbol{A}:\boldsymbol{B} = \sum_{ij} A_{ij} B_{ij}$, and the dimensionless form $\hat{\Phi}_2(\Delta, t)$ yields from division by $\langle \overline{\delta \boldsymbol{r} \delta \boldsymbol{r}}(\Delta, t) \rangle : \langle \overline{\delta \boldsymbol{r} \delta \boldsymbol{r}}(\Delta, t) \rangle$. $\hat{\Phi}_2(\Delta, t)$ also shows a slow decay in the time region $t \sim 10^{-1}$–1 μs, i.e., orientational diffusion of the protein fluctuates intrinsically.

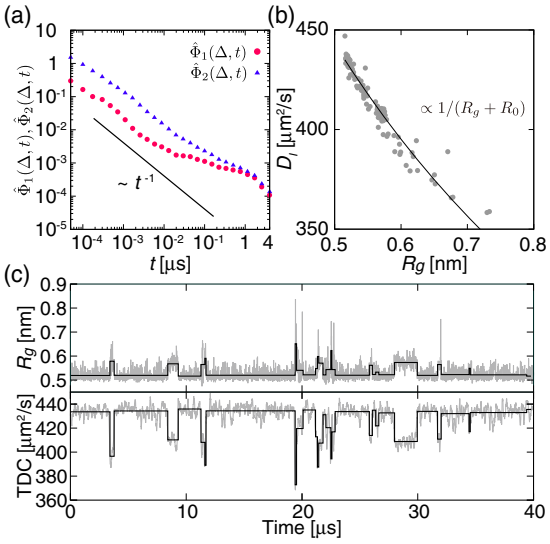

FIG. 3. Fluctuating diffusivity of Chignolin at 310 K and 0.1 MPa. (a) Normalized magnitude $\hat{\Phi}_1(\Delta, t)$ and orientation $\hat{\Phi}_2(\Delta, t)$ correlation functions. Forty-five divided trajectories were used with a lag time $\Delta = 50$ ps. (b) Correlation between the mean R_g and the instantaneous diffusion coefficient D_I in each diffusive state. (c) Time series of R_g and temporal diffusion coefficient (TDC). Thin lines represent unsmoothed original values every 10 ns. Thick lines represent mean R_g and D_I in each state, where $t = 100$ ns and $\Delta = 10$ ps were used to obtain the TDC.

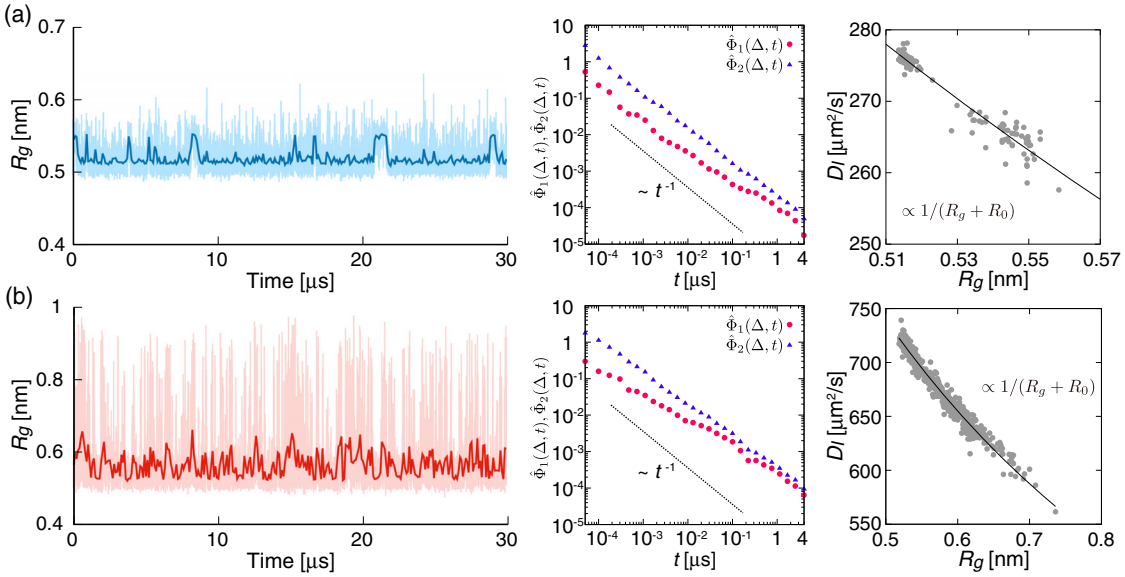

FIG. 4. Fluctuating diffusivity of Chignolin at different temperature and pressure conditions: (a) 280 K, 0.1 MPa and (b) 400 K, 400 MPa. Left: time series of R_g. Thin and thick lines represent unsmoothed original values every 1 ns and smoothed moving average with 100 ns averaging window, respectively. Middle: normalized magnitude $\hat{\Phi}_1(\Delta,t)$ and orientation $\hat{\Phi}_2(\Delta,t)$ correlation functions. Thirty-five divided trajectories were used with a lag time $\Delta = 50$ ps. Right: correlation between mean R_g and D_I in each diffusive state, where $t = 100$ ns and $\Delta = 10$ ps were used to obtain the TDC.

Both correlators $\Phi_1(\Delta,t)$ and $\Phi_2(\Delta,t)$ of Chignolin show a crossover at time $\tau_c \sim 1$ μs, corresponding to the lower crossover frequency in the PSD of R_g ($\sim 10^6$ Hz). Interestingly, the decays of $\Phi_1(\Delta,t)$ and $\Phi_2(\Delta,t)$ are similar to those of the flexible polymer model in dilute solutions, the Zimm model [35], incorporating hydrodynamic interactions between monomers (beads) of the polymer [67,68]. In the Zimm model, the correlation function $\langle 1/[R_g(t)R_g(0)]\rangle$ determines the magnitude of the diffusivity fluctuations [35], and the relaxation time is proportional to the solvent viscosity. Note that water molecules around biomolecules are known to exhibit subdiffusion [69–71]. Thus, the hydrodynamics interaction within the protein could be more complicated than that of the Zimm model.

To see a direct evidence that the instantaneous diffusivity intrinsically fluctuates with time, we obtained the TDC at time t^*,

$$D(t^*) = \frac{1}{2d\Delta(t-\Delta)} \int_{t^*}^{t^*+t-\Delta} [\boldsymbol{r}(t'+\Delta) - \boldsymbol{r}(t')]^2 dt'. \quad (4)$$

From the TDC, the transition times of the instantaneous diffusivity D_I were estimated with a statistical test [37,72] (Fig. S10). Note that D_I is assumed to be constant between the transition times. The time series of D_I and mean R_g in each diffusive state fluctuate synchronously. In particular, D_I decreases when the mean R_g increases [Fig. 3(c)]. A clear relation $D_I \propto 1/(R_g + R_0)$ can be seen in Fig. 3(b). Here, we assume the hydrodynamics radius of the protein is $R_H = R_g + R_0$ with $R_0 = 0.3$ nm, where we interpret R_0 as the hydration layer around the protein. Note that polymers in the Zimm model with longer chains, which form approximately spherical coils with a radius R_g, follow the SE-type relation $D \propto 1/R_g$, i.e., our form when $R_g \gg R_0$ [35,73].

The universal nature of the relation between D_I and R_g is underlined by MD simulations of Chignolin under two different temperature and pressure conditions (Fig. 4). At 280 K and 0.1 MPa, where the protein conformation changes little, R_g shows small fluctuations around $R_g = 0.51$–0.52 nm, but still R_g exhibits $1/f$ noise (Fig. S10), and the crossover frequency $\sim 10^6$ Hz corresponds to the crossover time ~ 1 μs of $\hat{\Phi}_1(\Delta,t)$. At 400 K and 400 MPa, where the protein exhibits frequent folding and unfolding, R_g shows significant fluctuations on a range of 0.5–1 nm. Now, the crossover time of $\hat{\Phi}_1(\Delta,t)$ is shorter, ~ 0.2 μs, which is related to the crossover frequency of the PSD of R_g at 5×10^6 Hz (Fig. S11). Notably, at both conditions, the relation $D_I \propto 1/(R_g + R_0)$ was observed with $R_0 = 0.2$ nm (280 K, 0.1 MPa) and $R_0 = 0.3$ nm (400 K, 400 MPa).

Conclusion.—Our study reveals a direct relation between the size fluctuations of proteins, encoded by the time dependence of the gyration radius R_g, and their instantaneous diffusivity D_I. Specifically, we uncovered the universal relationship $D_I \propto 1/(R_g + R_0)$, representing a time-local SE-type relation. We also demonstrated that the relaxation of the R_g dynamics is directly related to the conformational transitions in the protein energy landscape. Both features were studied for the protein Chignolin at different temperature and pressure conditions, as well as for

Villin and the WW domain of Pin1 (see Fig. S12). In particular, this analysis showed that the SE-type relation holds for both proteins with large and negligible R_g fluctuations. Note that the prefactors of the scaling $D_I = A/(R_g + R_0)$ for all proteins investigated here are the same order of magnitude of $k_B T/6\pi\eta$, and D_I is proportional to T/η (Fig. S13). The relatively small proteins analyzed here exhibit a crossover to stationary dynamics. We speculate that the instantaneous relationship $D_I \propto 1/(R_g + R_0)$ will also hold for larger proteins with more complex dynamics [74] (see also Fig. S14) and pronounced aging behavior [71], but this remains to be shown in supercomputing studies. Such a universal relation would be particularly interesting, as it shows that D_I for even highly unspherical proteins can be sufficiently characterized simply by R_g.

Our results provide a microscopic physical rationale for randomly fluctuating diffusivities as encoded in a range of recent modeling approaches. While here we focused on the internal protein dynamics, we speculate that the same SE-type relation will hold for proteins and other tracers moving in complex environments such as biological cells. There, on top of potential interactions with the cytoskeleton, tracers are typically not fully inert and may thus accumulate foreign molecules on their surface, leading to time-random instantaneous R_g and thus D_I [75]. Moreover, ongoing multimerization typical for many regulatory proteins may further randomize the tracers' D_I [31]. This also prompts the question of whether similar R_g-D_I relations will hold for tracers showing anomalous diffusion [75].

We thank Dr. Takashi Uneyama and Dr. Tomoshige Miyaguchi for fruitful discussion. This work was supported by Grant for Basic Science Research Projects from the Sumitomo Foundation and Grant No. ME1535/7-1 from German Research Foundation (DFG). A. M. also thanks the JSPS KAKENHI Grant No. JP20H03230 for support. R. M. also thanks the Foundation for Polish Science (FNP) for support.

*eiji.yamamoto@sd.keio.ac.jp

[1] M. E. Young, P. A. Carroad, and R. L. Bell, Biotechnol. Bioeng. **22**, 947 (1980).
[2] L. He and B. Niemeyer, Biotechnology Progress **19**, 544 (2003).
[3] M. T. Tyn and T. W. Gusek, Biotechnol. Bioeng. **35**, 327 (1990).
[4] B. Halle and M. Davidovic, Proc. Natl. Acad. Sci. U.S.A. **100**, 12135 (2003).
[5] A. P. Minton, J. Biol. Chem. **276**, 10577 (2001).
[6] R. Metzler, J.-H. Jeon, and A. G. Cherstvy, Biochim. Biophys. Acta **1858**, 2451 (2016).
[7] M. Javanainen, H. Martinez-Seara, R. Metzler, and I. Vattulainen, J. Phys. Chem. Lett. **8**, 4308 (2017).
[8] K. Weiß, A. Neef, Q. Van, S. Kramer, I. Gregor, and J. Enderlein, Biophys. J. **105**, 455 (2013).
[9] R. Yamamoto and A. Onuki, Phys. Rev. Lett. **81**, 4915 (1998).
[10] B. Wang, S. M. Anthony, S. C. Bae, and S. Granick, Proc. Natl. Acad. Sci. U.S.A. **106**, 15160 (2009).
[11] B. Wang, J. Kuo, S. C. Bae, and S. Granick, Nat. Mater. **11**, 481 (2012).
[12] A. Sergé, N. Bertaux, H. Rigneault, and D. Marguet, Nat. Methods **5**, 687 (2008).
[13] C. Manzo, J. A. Torreno-Pina, P. Massignan, G. J. Lapeyre, M. Lewenstein, and M. F. Garcia Parajo, Phys. Rev. X **5**, 011021 (2015).
[14] E. Yamamoto, A. C. Kalli, T. Akimoto, K. Yasuoka, and M. S. P. Sansom, Sci. Rep. **5**, 18245 (2015).
[15] J.-H. Jeon, M. Javanainen, H. Martinez-Seara, R. Metzler, and I. Vattulainen, Phys. Rev. X **6**, 021006 (2016).
[16] W. He, H. Song, Y. Su, L. Geng, B. J. Ackerson, H. B. Peng, and P. Tong, Nat. Commun. **7**, 11701 (2016).
[17] A. Weron, K. Burnecki, E. J. Akin, L. Solé, M. Balcerek, M. M. Tamkun, and D. Krapf, Sci. Rep. **7**, 5404 (2017).
[18] E. Yamamoto, T. Akimoto, A. C. Kalli, K. Yasuoka, and M. S. P. Sansom, Sci. Adv. **3**, e1601871 (2017).
[19] T. J. Lampo, S. Stylianidou, M. P. Backlund, P. A. Wiggins, and A. J. Spakowitz, Biophys. J. **112**, 532 (2017).
[20] A. G. Cherstvy, O. Nagel, C. Beta, and R. Metzler, Phys. Chem. Chem. Phys. **20**, 23034 (2018).
[21] P. Massignan, C. Manzo, J. A. Torreno-Pina, M. F. García-Parajo, M. Lewenstein, and G. J. Lapeyre, Phys. Rev. Lett. **112**, 150603 (2014).
[22] M. V. Chubynsky and G. W. Slater, Phys. Rev. Lett. **113**, 098302 (2014).
[23] T. Uneyama, T. Miyaguchi, and T. Akimoto, Phys. Rev. E **92**, 032140 (2015).
[24] T. Akimoto and E. Yamamoto, Phys. Rev. E **93**, 062109 (2016).
[25] T. Miyaguchi, T. Akimoto, and E. Yamamoto, Phys. Rev. E **94**, 012109 (2016).
[26] A. G. Cherstvy and R. Metzler, Phys. Chem. Chem. Phys. **18**, 23840 (2016).
[27] A. V. Chechkin, F. Seno, R. Metzler, and I. M. Sokolov, Phys. Rev. X **7**, 021002 (2017).
[28] N. Tyagi and B. J. Cherayil, J. Phys. Chem. B **121**, 7204 (2017).
[29] R. Jain and K. L. Sebastian, Phys. Rev. E **98**, 052138 (2018).
[30] A. Sabri, X. Xu, D. Krapf, and M. Weiss, Phys. Rev. Lett. **125**, 058101 (2020).
[31] M. Hidalgo-Soria and E. Barkai, Phys. Rev. E **102**, 012109 (2020).
[32] V. Sposini, D. Grebenkov, R. Metzler, G. Oshanin, and F. Seno, New J. Phys. **22**, 063056 (2020).
[33] E. Barkai and S. Burov, Phys. Rev. Lett. **124**, 060603 (2020).
[34] W. Wang, F. Seno, I. M. Sokolov, A. V. Chechkin, and R. Metzler, New J. Phys. **22**, 083041 (2020).
[35] T. Miyaguchi, Phys. Rev. E **96**, 042501 (2017).
[36] S. Honda, T. Akiba, Y. S. Kato, Y. Sawada, M. Sekijima, M. Ishimura, A. Ooishi, H. Watanabe, T. Odahara, and K. Harata, J. Am. Chem. Soc. **130**, 15327 (2008).
[37] See Supplemental Material at http://link.aps.org/supplemental/10.1103/PhysRevLett.126.128101 for details

of MD simulations, analysis, and additional figures, which includes Refs. [38–50].
[38] J. Kubelka, T. K. Chiu, D. R. Davies, W. A. Eaton, and J. Hofrichter, J. Mol. Biol. **359**, 546 (2006).
[39] R. Ranganathan, K. P. Lu, T. Hunter, and J. P. Noel, Cell **89**, 875 (1997).
[40] M. J. Abraham, T. Murtola, R. Schulz, S. Páll, J. C. Smith, B. Hess, and E. Lindahl, SoftwareX **1–2**, 19 (2015).
[41] H. Okumura, Proteins **80**, 2397 (2012).
[42] H. J. C. Berendsen, J. P. M. Postma, W. F. van Gunsteren, A. DiNola, and J. R. Haak, J. Chem. Phys. **81**, 3684 (1984).
[43] G. Bussi, T. Zykova-Timan, and M. Parrinello, J. Chem. Phys. **130**, 074101 (2009).
[44] K. Lindorff-Larsen, S. Piana, K. Palmo, P. Maragakis, J. L. Klepeis, R. O. Dror, and D. E. Shaw, Proteins **78**, 1950 (2010).
[45] W. L. Jorgensen, J. Chandrasekhar, J. D. Madura, R. W. Impey, and M. L. Klein, J. Chem. Phys. **79**, 926 (1983).
[46] B. Hess, H. Bekker, H. J. C. Berendsen, and J. G. E. M. Fraaije, J. Comput. Chem. **18**, 1463 (1997).
[47] U. Essmann, L. Perera, M. L. Berkowitz, T. Darden, H. Lee, and L. G. Pedersen, J. Chem. Phys. **103**, 8577 (1995).
[48] A. Mitsutake and H. Takano, Biophys. Rev. **10**, 375 (2018).
[49] Y. Naritomi and S. Fuchigami, J. Chem. Phys. **134**, 065101 (2011).
[50] H. Durchschlag and P. Zipper, J. Appl. Crystallogr. **30**, 1112 (1997).
[51] I. E. T. Iben, D. Braunstein, W. Doster, H. Frauenfelder, M. K. Hong, J. B. Johnson, S. Luck, P. Ormos, A. Schulte, P. J. Steinbach, A. H. Xie, and R. D. Young, Phys. Rev. Lett. **62**, 1916 (1989).
[52] M. Takano, T. Takahashi, and K. Nagayama, Phys. Rev. Lett. **80**, 5691 (1998).
[53] H. Yang, G. Luo, P. Karnchanaphanurach, T. M. Louie, I. Rech, S. Cova, L. Xun, and X. S. Xie, Science **302**, 262 (2003).
[54] E. Yamamoto, T. Akimoto, Y. Hirano, M. Yasui, and K. Yasuoka, Phys. Rev. E **89**, 022718 (2014).
[55] M. Niemann, H. Kantz, and E. Barkai, Phys. Rev. Lett. **110**, 140603 (2013).
[56] S. Sadegh, E. Barkai, and D. Krapf, New J. Phys. **16**, 113054 (2014).
[57] N. Leibovich and E. Barkai, Phys. Rev. Lett. **115**, 080602 (2015).
[58] H. Takano and S. Miyashita, J. Phys. Soc. Jpn. **64**, 3688 (1995).
[59] H. Hirao, S. Koseki, and H. Takano, J. Phys. Soc. Jpn. **66**, 3399 (1997).
[60] A. Mitsutake, H. Iijima, and H. Takano, J. Chem. Phys. **135**, 164102 (2011).
[61] A. Mitsutake and H. Takano, J. Chem. Phys. **143**, 124111 (2015).
[62] Y. He, S. Burov, R. Metzler, and E. Barkai, Phys. Rev. Lett. **101**, 058101 (2008).
[63] R. Metzler, J.-H. Jeon, A. G. Cherstvy, and E. Barkai, Phys. Chem. Chem. Phys. **16**, 24128 (2014).
[64] T. Miyaguchi and T. Akimoto, Phys. Rev. E **83**, 031926 (2011).
[65] T. Miyaguchi and T. Akimoto, Phys. Rev. E **83**, 062101 (2011).
[66] T. Akimoto and E. Yamamoto, J. Stat. Mech. (2016) 123201.
[67] B. H. Zimm, J. Chem. Phys. **24**, 269 (1956).
[68] D. L. Ermak and J. A. McCammon, J. Chem. Phys. **69**, 1352 (1978).
[69] E. Yamamoto, T. Akimoto, M. Yasui, and K. Yasuoka, Sci. Rep. **4**, 4720 (2014).
[70] P. Tan, Y. Liang, Q. Xu, E. Mamontov, J. Li, X. Xing, and L. Hong, Phys. Rev. Lett. **120**, 248101 (2018).
[71] D. Krapf and R. Metzler, Phys. Today **72**, No. 9, 48 (2019).
[72] T. Akimoto and E. Yamamoto, Phys. Rev. E **96**, 052138 (2017).
[73] M. Doi and S. F. Edwards, *The Theory of Polymer Dynamics* (Oxford University Press, Oxford, 1988).
[74] X. Hu, L. Hong, M. D. Smith, T. Neusius, X. Cheng, and J. C. Smith, Nat. Phys. **12**, 171 (2016).
[75] F. Etoc, E. Balloul, C. Vicario, D. Normanno, D. Liße, A. Sittner, J. Piehler, M. Dahan, and M. Coppey, Nat. Mater. **17**, 740 (2018).